C. R. Chimie 13 (2010) 737–746

Contents lists available at ScienceDirect

Comptes Rendus Chimie

www.sciencedirect.com

Account/Revue

From extended solids to nano-scale actinide clusters

Peter C. Burns

Department of Civil Engineering and Geological Sciences and the Department of Chemistry and Biochemistry, University of Notre Dame, 156, Fitzpatrick Hall, Notre Dame, IN 46556, USA

ARTICLE INFO

Article history:
Received 2 December 2009
Accepted after revision 28 January 2010
Available online 24 March 2010

Keywords:
Uranyl
Uranium
Actinide
Cluster
Topology

ABSTRACT

Selected highlights of more than a decade of research efforts concerning the structural chemistry of actinyl materials at the University of Notre Dame is reviewed, with an emphasis on complex topological arrangements of polyhedra to form extended structures and frameworks. Earlier work focused on structures of uranyl minerals and synthetic compounds, with increasing emphasis on neptunyl materials and the importance of cation–cation interactions in their structural details and properties. Much of the research over the past 5 years has examined a growing family of nano-scale clusters of uranyl peroxide polyhedra containing from 16 to 60 polyhedra. These clusters contain topological squares, pentagons and hexagons, and six have adopted fullerene topologies with 12 pentagons and an even number of hexagons.

1. Introduction

A fascinating aspect of the actinide elements is their incredible solid-state structural diversity when they are in higher oxidation states. With only a few exceptions, the topologies of structures containing trivalent and tetravalent actinides are dominated by their regular coordination polyhedra and uninspired parallels with structures common in other parts of the periodic table, especially the lanthanides. Higher valence actinides shoulder aside this normalcy, regularly adopting structural topologies unique in chemistry [1,2].

The details of higher valence actinide (pentavalent and hexavalent) coordination polyhedra are the underlying cause of the myriad of unique structural topologies. The cations are contained within linear (or slightly bent) actinyl ions, in which the cation is bonded to two atoms of O, resulting in an ion with a formal valence of +1 or +2 [3]. The bonds within the actinyl ions are very strong [3]. The residual valence of the actinyl ion and the radius of the central cation are consistent with coordination by four to six ligands that are arranged at the equatorial vertices of square, pentagonal and hexagonal bipyramids. The apical ligands of these bipyramids are the O atoms of the actinyl ions and their bonding requirements are mostly met by their bonds to the actinyl cations alone [1,2,4]. In contrast, where the equatorial ligands are O or OH, they require significant additional bonding to satisfy their bonding requirements. The result is linkage of actinyl polyhedra with other actinyl polyhedra, or other cation-centered polyhedra, forming extended and often highly complex structures [1,2].

The bond-valence approach [5–7] is useful in rationalizing solid-state structures containing actinides in higher oxidation states [4]. In this approach, the bond-valence associated with a bond is a unique function of the bond length and is calculated using parameters that are empirically fit to well-known structures [4,6,7]. Considering the $(UO_2)^{2+}$ uranyl ion and the $(NpO_2)^{1+}$ neptunyl ion, the typical bond-valences associated with the strong actinyl ion bonds are about 1.7 and 1.6 valence units (*vu*), respectively [1,2,4]. The bond-valence strengths of the much weaker interactions with equatorial O, OH and H_2O are in the range of 0.3 to 0.6 *vu* in most structures [1,2,4]. As such, linkages between actinyl polyhedra are dominantly through the equatorial ligands.

E-mail address: pburns@nd.edu.

1631-0748/$ – see front matter © 2010 Académie des sciences. Published by Elsevier Masson SAS. All rights reserved.
doi:10.1016/j.crci.2010.01.014

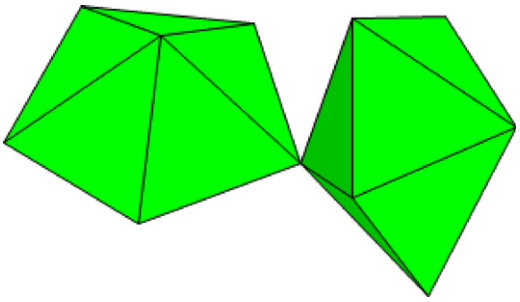

Fig. 1. Polyhedral representation of a cation–cation interaction in which an O atom of one actinyl ion is also an equatorial ligand of another actinyl bipyramid.

The slightly weaker bonds within the Np^{5+} neptunyl ion, relative to U^{6+} uranyl, favor cation–cation interactions. In these interactions, an O atom of an actinyl ion is also the equatorial vertex of the bipyramid about another actinyl ion (Fig. 1). Such interactions were first found by Sullivan et al. in 1961 [8] and are quite unusual in the case of hexavalent actinide cations, but are much more common for pentavalent cations [2,9]. Cation–cation interactions are emerging as a connectivity theme in about 50% of structures containing pentavalent actinides [2,9]. They only occur in about 2% of U^{6+} uranyl structures [1], but have recently been reported in several structures containing U^{5+} [10–16].

Our studies of actinide crystal chemistry began in 1996 with an emphasis on uranyl minerals [17]. There are approximately 200 known uranyl minerals that are mostly found in the oxidized portions of U ore deposits [18]. Interest in uranyl minerals stems from their importance in the transport of actinides in contaminated soils and groundwater [19–21], for understanding the origin and history of U deposits [18] and the behavior of nuclear waste in a geological repository [18,22–29]. Our efforts examined mineral specimens from many localities worldwide and increased the number of well-determined uranyl mineral structures by 70% [1]. Our ongoing research concerning uranyl crystal chemistry expanded to include synthetic materials a decade ago and has since led to studies of polyoxometalate clusters based on uranyl ions [30–34] as well as studies of transuranium clusters [35] and solid-state chemistry [2,36–44]. Here, we summarize aspects of our research in actinide structural chemistry, with an emphasis on formation of complex cluster topologies.

2. Extended topologies containing U^{6+}, Np^{5+} or Np^{6+}

Burns et al. published a structural hierarchy of inorganic uranyl compounds in 1996 in which 180 structures were organized and described on the bases of the connectivity of their cation-centered polyhedra of higher valence [17]. The hierarchy was updated, following publication of many new structures, by Burns in 2005 [1], who considered 368 inorganic structures. The structural units defined by the polyhedra of higher bond-valence were categorized as isolated polyhedra (8), finite clusters (43), chains (57), sheets (204) and frameworks (56). The dominance of sheets arises from the uneven distribution of bond-strengths within the uranyl polyhedra (see above). Except in the case of cation–cation interactions, linkages are through equatorial vertices of the bipyramids.

Forbes et al. created a structural hierarchy for Np^{5+} and Np^{6+} compounds in 2008 [2] that is broadly similar to that for uranyl compounds. Forty-three Np^{5+} compounds containing isolated polyhedra (2), finite clusters of polyhedra (1), chains of polyhedra (12), sheets of polyhedra (16) and frameworks of polyhedra (12) were discussed. In stark contrast to structures containing U^{6+}, in which cation–cation interactions are rare, this mode of connectivity occurs in 18 of the 43 Np^{5+} compounds. Forbes et al. [2] also arranged 16 Np^{6+} compounds, none of which contain cation–cation interactions, in a hierarchy that is heavily dominated by chains and sheets. The topologies of Np^{6+} structural units are often similar to their U^{6+} analogues, whereas Np^{5+} structural topologies often depart significantly from those of U^{6+}.

Interesting examples of actinyl compounds we have studied belonging to each of the major structural classes are shown in Figs. 2–4. Topological comparisons within the cluster and chain groups are facilitated by a graphical approach in which each uranyl bipyramid is represented by a black circle and other polyhedra are shown as white circles (e.g., Fig. 2b and d) [1]. Lines between these circles give information on the connections between them in the corresponding structure. Specifically, a single line represents a shared polyhedral element, a double line indicates the corresponding polyhedra share an edge and a triple line denotes the sharing of a polyhedral face. Where cation–cation interactions are present, the lines in the graph that connect nodes corresponding to cation–cation interactions are designated with an arrow, where the arrow points away from the donor of the cation–cation interaction, in the direction of the acceptor [2] (Fig. 3e).

The cluster shown in Fig. 2a consists of a uranyl pentagonal bipyramid in which each of the equatorial O atoms belong either to one bidentate or three monodentate sulfate tetrahedra. This cluster, which has been found in three purely inorganic uranyl compounds where the charge of the cluster is balanced by Na and/or K atoms [45–47], includes the relatively rare sharing of an equatorial edge of the bipyramid with a sulfate tetrahedron. In contrast, the cluster shown in Fig. 2c contains two uranyl pentagonal bipyramids that are coordinated by eight monodentate molybdate tetrahedra, with two tetrahedra bridging between the bipyramids. This cluster has been found in two compounds where the charge of the cluster is balanced by interstitial low-valence cations [48,49].

From a topological perspective, one of the most complex chains of uranyl polyhedra occurs in the structure of the mineral uranopilite (Fig. 2e), $[(UO_2)_6(SO_4)O_2(OH)_6(H_2O)_6]$ [50]. The chain contains clusters of six edge-sharing uranyl pentagonal bipyramids. These clusters are linked through sulfate tetrahedra such that each tetrahedron shares its four vertices with four different uranyl polyhedra, two of which are in each cluster. In uranyl compounds, it is more common to find chains where uranyl bipyramids are linked by

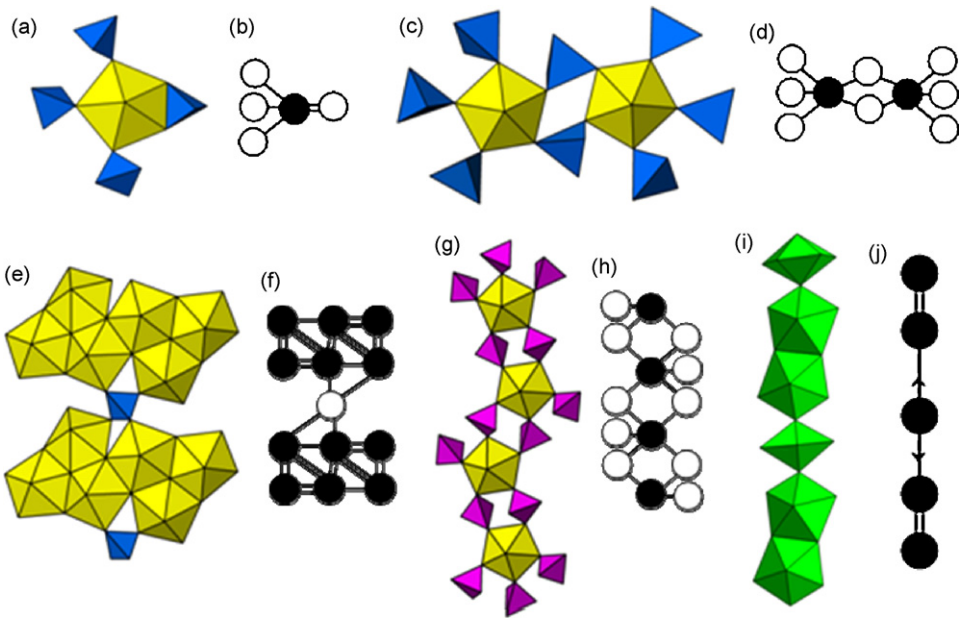

Fig. 2. Examples of cluster and chain topologies of U^{6+} uranyl (yellow) and Np^{5+} neptunyl (green) polyhedra. (a,b) a uranyl sulfate cluster [45–47], (c,d) a uranyl molybdate cluster [48,49], (e,f) a uranyl sulfate chain found in the mineral uranopilite [50], (g,h) a uranyl chromate chain [51], (i,j) a chain of Np^{5+} neptunyl ions containing cation–cation interactions [39].

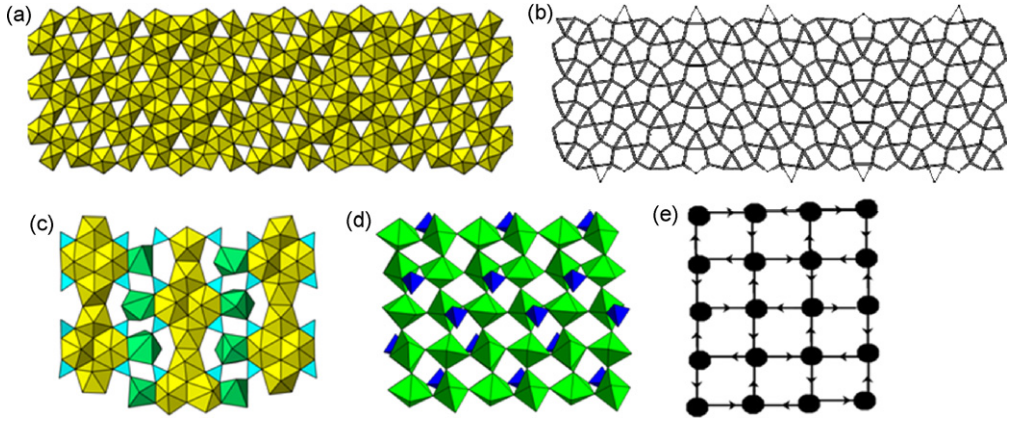

Fig. 3. Illustrations of sheets of polyhedra that occur in uranyl (yellow) and neptunyl (green) compounds. (a) the sheet of uranyl square and pentagonal bipyramids in the structure of wölsendorfite [52], (b) the wölsendorfite sheet anion-topology, (c) the sheet of uranyl pentagonal and hexagonal bipyramids, carbonate triangles, and M^{3+} polyhedra in the structure of bijvoetite [53], (d) a sheet of Np^{5+} neptunyl polyhedra and sulfate tetrahedra that exhibits extensive cation–cation interactions [41], (e) graphical representation of the sheet shown in (d), with the donor-acceptor cation–cation interactions shown by arrows.

sharing their equatorial vertices with tetrahedra, such as in the uranyl chromate chain shown in Fig. 2g [51].

Np^{5+} neptunyl polyhedra are often linked into chains, and in the absence of cation–cation interactions, these can be topologically similar to those found in U^{6+} compounds [36]. Where cation–cation interactions are present within the chain, very different topologies result, as shown in Fig. 1i. This structure contains dimers of edge-sharing pentagonal bipyramids that are linked into a chain by cation–cation interactions with a third neptunyl bipyramid [39]. This chain contains a neptunyl ion that is oriented approximately parallel to the chain length, a feature that appears to occur only where cation–cation interactions exist.

There are many examples of sheets of uranyl polyhedra with complex topologies and also of uranyl polyhedra and various additional oxyanions. We have adopted a hierarchical arrangement for sheets that is based upon the topological arrangement of anions in these sheets [1,17]. The sheet anion topology is a two-dimensional sheet of polygons that represents the projection of the positions of two- or higher-connected anions within the sheet, connected with lines where the anions are close enough together to occur in a single polyhedron (Fig. 3b). The

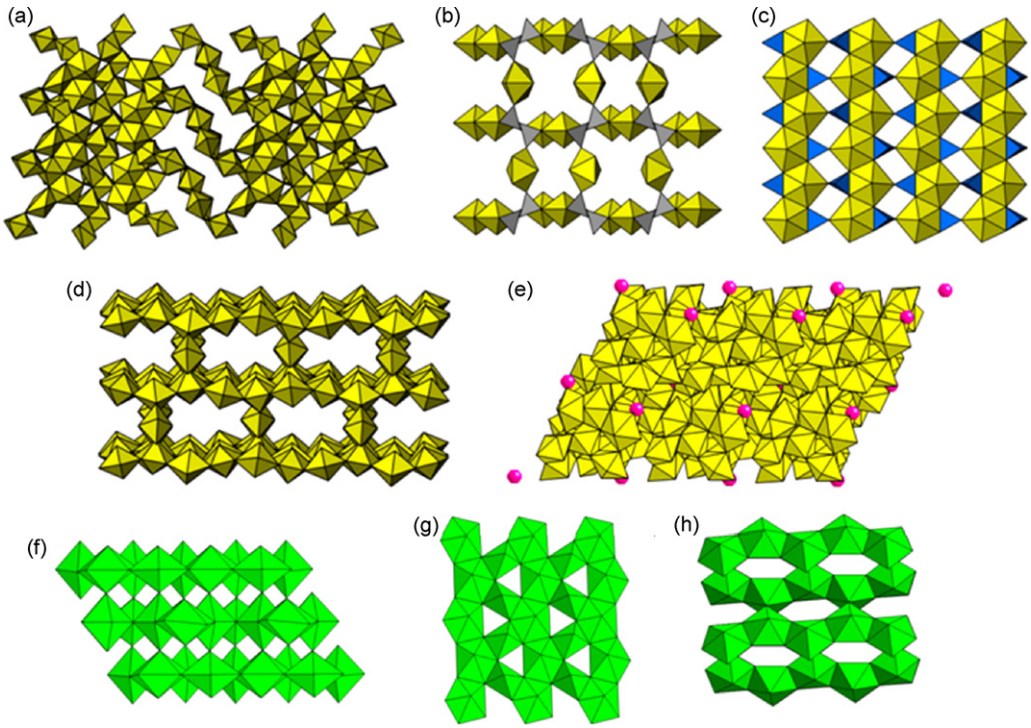

Fig. 4. Frameworks of polyhedra. (a) a Pb uranyl oxide hydrate [55], (b,c) a uranyl phosphate [56], (d,e) frameworks of uranyl polyhedra containing cation–cation interactions [57], (f,g) framework of Np^{5+} neptunyl polyhedra in Np_2O_5 including cation–cation interactions [42], (h) Np^{5+} neptunyl polyhedra in a Na neptunyl oxide hydrate [58].

utility of this approach is that sheets of polyhedra that appear rather different often have the same underlying anion topology and relationships between chemically disparate sheets are more apparent [17].

No sheets of uranyl polyhedra are known that contain cation–cation interactions within the sheet, but such linkages occur in the case of Np^{5+} neptunyl polyhedra. A graphical approach is adopted where cation–cation interactions are present, similar to that used for clusters and chains, illustrating the locations and directional aspects of the cation–cation interactions (Fig. 3e).

More than a dozen uranyl minerals and several synthetic compounds contain sheets that consist only of uranyl bipyramids, but several different topologies exist. The most complex of these is from the structure of wölsendorfite, $Pb_{6.16}Ba_{0.36}[(UO_2)_{14}O_{19}(OH)_4](H_2O)_{12}$ (Fig. 3a) [52]. This extraordinarily complex topology has a primitive repeat distance of 56 Å, despite its construction from only two types of polyhedra, uranyl square and pentagonal bipyramids. This topology may be regarded as a modular structure formed from slabs of much simpler known topologies [52], although the factors that stabilize it are unclear.

The mineral bijvoetite, $[M^{3+}(H_2O)_{25}(UO_2)_{16}O_8(OH)_8(CO_3)_{16}](H_2O)_{14}$ (M^{3+} = Y, rare-earth-elements), presents an interesting complex sheet that contains two types of uranyl bipyramids, carbonate triangles and irregular polyhedra occupied by Y and rare-earth-elements [53] (Fig. 3c). There are chains of edge-sharing uranyl pentagonal and hexagonal bipyramids, with carbonate triangles sharing edges with the hexagonal bipyramids. Adjacent sheets are connected through the rare-earth-element polyhedra. The sheet is a rare example of a topology containing three different cations.

The structure of $(NpO_2)_2(SO_4)(H_2O)_4$ contains a sheet of neptunyl bipyramids in which the connectivity is dominated by cation–cation interactions [41] (Fig. 3d,e). This sheet containing pentavalent neptunium is radically distinct from uranyl sulfate sheets, none of which contain cation–cation interactions. As shown by the corresponding graph (Fig. 3e), neptunyl ions in the sheet in $(NpO_2)_2(SO_4)(H_2O)_4$ donate two cation–cation interactions as well as accepting two cation–cation interactions. The neptunyl ions are oriented parallel to the sheet, a feature that is restricted to sheets containing cation–cation interactions. This complex cation–cation interaction dominated connectivity was termed a cationic net by Krot and Grigoriev [54].

Framework structures containing U^{6+} polyhedra account for about 15% of structures. One of the more interesting frameworks was found for $Pb_2(H_2O)[(UO_2)_{10}UO_{12}(OH)_6(H_2O)_6]$ [55] (Fig. 4a), which consists of slabs of distorted uranyl square bipyramids, more regular uranyl pentagonal bipyramids and U^{6+} in distorted octahedral coordination with bond lengths ranging from 1.98 to 2.08 Å. These slabs form a framework with voids that contain charge-balancing Pb cations. Some framework structures have strong sheet-like characteristics, such as the uranyl phosphate framework of $(UO_2)_3(PO_4)_2(H_2O)_4$ [56] (Fig. 4b,c). This compound contains sheets of uranyl

pentagonal bipyramids and phosphate tetrahedra that have the uranophane anion topology (Fig. 4c), but the sheets are connected into a framework through uranyl ions located in the interlayer regions (Fig. 4b). These uranyl ions include apical ligands of phosphate tetrahedra as equatorial ligands of their bipyramids.

Occasionally, a framework structure with uranyl ions contains cation–cation interactions. Two examples of this are the structures of $Sr_5(UO_2)_{20}(UO_6)_2O_{16}(OH)_6(H_2O)_6$ and $Cs(UO_2)_9U_3O_{16}(OH)_5$ [57] (Fig. 4d,e). The first of these contains sheets of uranyl square bipyramids, uranyl pentagonal bipyramids and distorted octahedra containing U^{6+} and these are connected into a framework through cation–cation interactions donated by sheet uranyl ions and accepted by a dimer of edge-sharing uranyl pentagonal bipyramids in the interlayer. The compound $Cs(UO_2)_9U_3O_{16}(OH)_5$ consists of a complex framework containing distorted U^{6+} octahedra, pentagonal bipyramids and cation–cation interactions that extend between uranyl ions of pentagonal bipyramids.

Considering the 12 inorganic Np^{5+} compounds with framework structures examined in the recent structural hierarchy [2], 10 of these contain cation–cation interactions. The binary oxide Np_2O_5 [42] contains abundant cation–cation interactions (Fig. 4f,g). The framework consists of both neptunyl square and pentagonal bipyramids connected into layers with the same anion topology as the sheets in the uranophane group of minerals. However, unlike in uranyl minerals, these layers contain cation–cation interactions. Cation–cation interactions also tightly link the layers into a three-dimensional framework. Np_2O_5 undergoes antiferromagnetic ordering at 22 K. In contrast, the compound $Na[NpO_2(OH)_2]$ contains a more open framework that consists dominantly of chains of edge-sharing neptunyl pentagonal bipyramids (Fig. 4h) [58]. These chains are connected to identical adjacent chains through cation–cation interactions. This compound undergoes antiferromagnetic ordering at 19 K. It has been suggested that cation–cation interactions in Np^{5+} compounds provide a super-exchange pathway, facilitating magnetic ordering [42,43,58].

3. Uranyl peroxides

Studtite, $(UO_2)(O_2)(H_2O)_2(H_2O)_2$, and its lower hydrate version metastudtite are the only known peroxide minerals [59,60]. Our interest in uranyl peroxides began in 2002, spurred by the oddity of this mineral and its significance in nuclear waste isolation. It forms in U deposits in close contact with U minerals owing to the buildup of peroxide generated by alpha radiolysis in thin films of water [61]. Studtite was found as an alteration product of nuclear materials following the Chernobyl accident [62] and on used nuclear fuel in contact with water [63,64]. In studtite, uranyl hexagonal bipyramids in which two *trans* edges are occupied by peroxide share these peroxide edges, forming chains (Fig. 5). Hydrogen bonds emanating from H_2O located at the remaining two equatorial vertices of the bipyramids, as well as interstitial H_2O groups, links these chains into an extended structure.

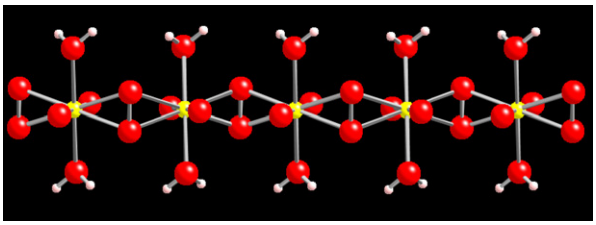

Fig. 5. The chain of uranyl peroxide hexagonal bipyramids that is the basis of the structure of the mineral studtite [72].

The non-mineral analogue of studtite, uranyl peroxide hydrate, has been known for decades and is important in U extraction processes, although its crystal structure was unknown prior to our work. Under acidic conditions, the phase is insoluble and addition of peroxide to a uranyl-bearing aqueous solution results in rapid precipitation. Little was known about actinyl peroxide complexes in alkaline aqueous solutions, but a report published four decades ago indicated brightly colored crystals grew from such solutions containing uranyl [65]. We quickly learned that uranyl is highly soluble in alkaline solutions containing peroxide and that these solutions are brightly colored in shades of yellow, orange and dark red. Where Na is added, the phase $Na_4[(UO_2)(O_2)_3](H_2O)_9$, which was the only inorganic actinide peroxide structure reported prior to our research [66], crystallizes in minutes. Other solution compositions produced crystals only after weeks or months.

The first novel compound we isolated from alkaline aqueous uranyl peroxide solutions was not only unexpected, it challenged our understanding of uranyl crystal chemistry (Fig. 6a). It consists of isolated clusters of 24 uranyl hexagonal bipyramids, each of which contained two peroxide groups that defined *cis* equatorial edges of the bipyramid, with an additional edge defined by two hydroxyl groups [30]. These 24 compositionally identical bipyramids share their peroxide edges, as well as the edge defined by two hydroxyl groups, with three adjacent bipyramids. The U–O_2–U and U–$(OH)_2$–U dihedral angles are strongly bent and the 24 bipyramids link to form a closed cluster designated U_{24} (Fig. 6a,d). (Hereafter, clusters of uranyl polyhedra will be designated U_n, where n indicates the number of polyhedra. Ring-shaped clusters will include the designation "R", as in U_{nR}). The uranyl ions in this cluster are roughly perpendicular to the wall, and the relatively unreactive O atoms of these ions protrude into the cluster and extend away from the cluster.

We used small angle X-ray scattering (SAXS) to study the U_{24} system through time [30]. Data were collected for solutions ranging in age from a few days to 180 days. The 180-day-old solution was determined to be essentially monodisperse U_{24}, verifying that this cluster can persist in solution for extended periods and also indicating that under the alkaline aqueous solution conditions, the U_{24} cluster is soluble. The data was well modelled using a spherical-shell model and the derived dimensions of the cluster in solution matched well with those derived from diffraction data collected for single crystals containing U_{24}. Data collected after a few days and weeks could not be

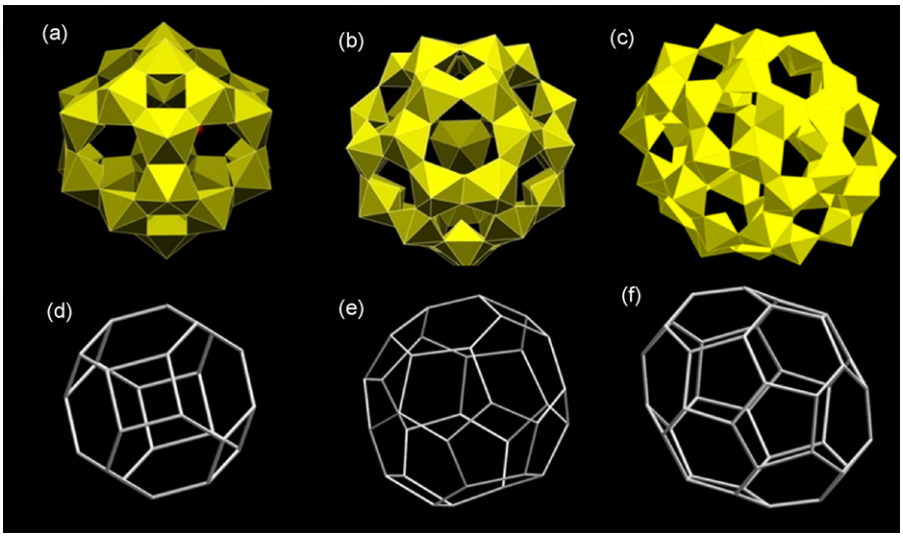

Fig. 6. Clusters of uranyl peroxide hexagonal bipyramids containing topological squares. Shown are the polyhedral representations of the clusters (in yellow), and the topological graphs [30,31]. (a,d) U_{24}, (b,e) U_{32}, (c,f) U_{40}.

readily interpreted on the basis of a single shape and size, which suggests multiple clusters may have been present in solution. Current studies are emphasizing the evolution of the clusters in solution through time.

We reasoned that the discovery of U_{24} directed us to a family of polyoxometalate clusters and commenced to search for additional topologies. This was not initially guided by knowledge of the mechanisms of formation of U_{24}, as even now such insights are only developing. Rather, we adopted a systematic combinatorial approach. Quickly, the closed U_{28} and U_{32} clusters were isolated [30] (Figs. 6b, 7b). This early stage of rapid discovery halted abruptly only a few months after isolation of U_{24}. Continued efforts for more than a year turned up nothing new, until experiments using organic cations finally produced U_{40} and U_{50} [31] (Figs. 6c, 7h).

More than 10,000 synthesis experiments were conducted in search of conditions favorable for the formation of uranyl peroxide clusters. To date, we have reported clusters with a dozen unique topologies. All of these contain the uranyl ion as well as peroxide and some also contain hydroxyl groups. All uranyl ions are present in hexagonal bipyramidal polyhedra with either two *cis* peroxide edges or three peroxide edges. The 12 topologies that have been reported consist of closed clusters (approximately spherical or elliptical) and open bowl-shaped and crown-shaped clusters. These are illustrated in Figs. 6–8, where polyhedral representations and connectivity graphs may be found. In the connectivity graphs, vertices give the location of uranyl polyhedra and lines represent shared edges between polyhedra (note that this graphical representation is distinct from that used earlier for clusters, chains and sheets, where a shared polyhedral edge is designated by a double line). The topological details are readily apparent in the connectivity graphs and lead to subdivisions based upon the geometric shapes of the topological elements. Unlike C-based clusters, topological squares are common, a feature that leads to considerable topological diversity in uranyl clusters.

3.1. Bowl and crown-shaped clusters

We have reported the synthesis and characterization of the structures of three open clusters of uranyl peroxide polyhedra [34]. One has an interesting bowl shape, whereas two resemble crowns (Fig. 8). In general, closed clusters might be expected to be more stable than open clusters. This is because the uranyl ion O atoms that delineate the inner and outer surfaces of closed clusters are relatively unreactive. Clusters that are not closed have polyhedra with unshared peroxide or hydroxyl ligands, which requires significant linkages to counterions for stabilization.

The smallest extended cluster we have found, U_{16}, is bowl-shaped (Fig. 8a). The base corresponds to a topological square and the sides to hexagons, of which there are four (Fig. 8d). This topology can be directly extracted from the U_{24} topology of squares and hexagons, but here incorporation of Cs within the cluster appears to hold it open, preventing closure into a U_{24} cluster [34]. U_{16} demonstrates the potentially important role of counter ions that are contained within the cluster in influencing the details of their topology.

The crown-shaped U_{20R} and U_{24R} clusters shown in Fig. 8 have unique attributes. These are the only clusters we have found to date with crown topologies and they are also unusual in that they consist of a single type of topological polygon. U_{20R} is built only from topological pentagons and these are linked through a single connection to form the crown structure. U_{24R} has only topological hexagons and these share edges about the circumference of the crown. The U_{20R} cluster can be extracted from the larger closed U_{28} cluster (Fig. 7b,e), although in the closed cluster all of the polyhedra contain three peroxide edges. Both uranyl diperoxide and triperoxide polyhedra occur in

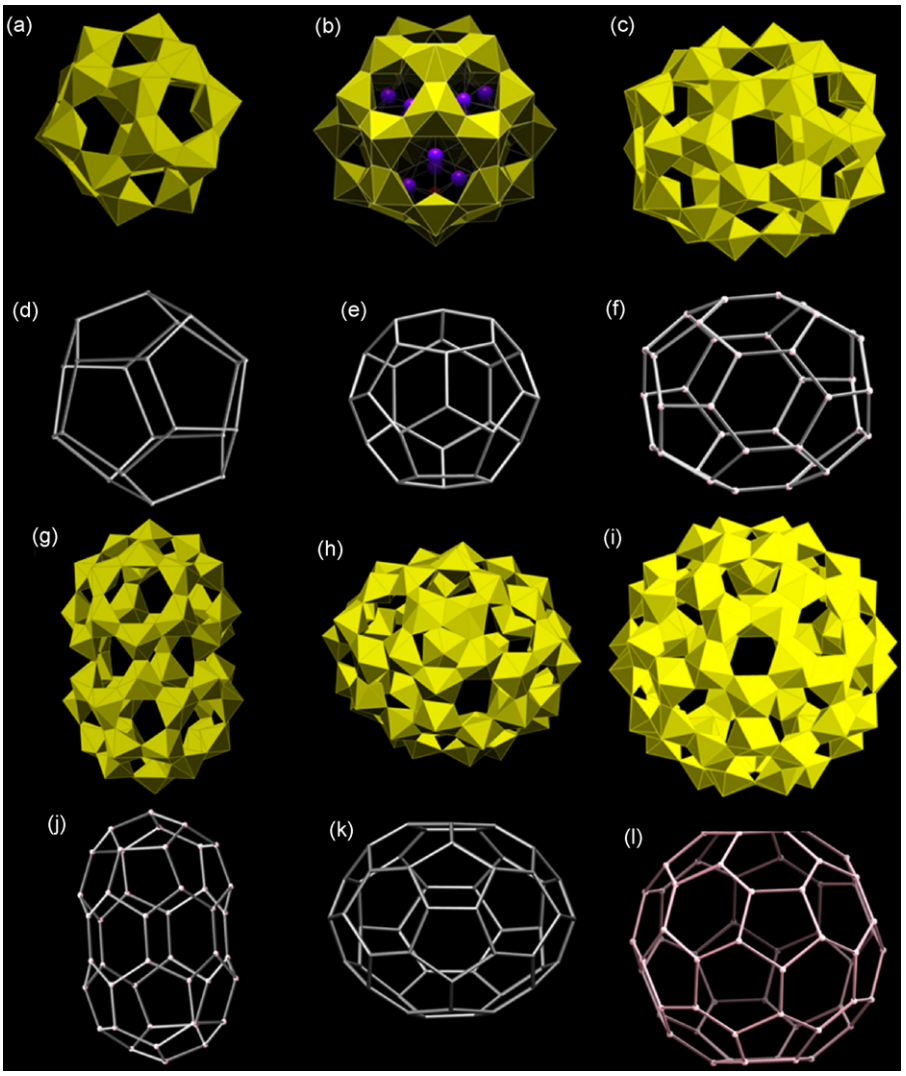

Fig. 7. Polyhedral and graphical representations of clusters of uranyl peroxide polyhedra with fullerene topologies [30,31,33,70]. (a,d) U_{20}, (b,e) U_{28}, (c,f) U_{36}, (g,j) U_{44}, (h,k) U_{50}, (i,l) U_{60}.

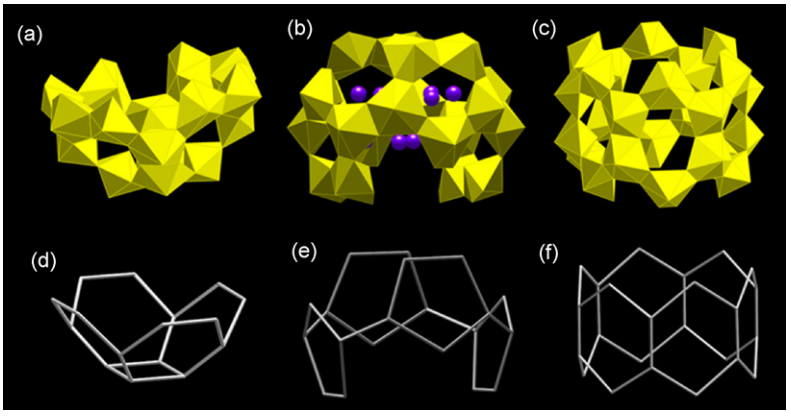

Fig. 8. Clusters of uranyl peroxide polyhedra with bowl (a) and crown (b,c) shapes [34]. (a,d) U_{16}, (b,e) U_{20R}, (c,f) U_{24R}.

the crown-shaped clusters U_{20R} and U_{24R}, as well as in the bowl-shaped U_{16}, which suggests tuning solutions to contain both of these complexes may favor formation of complex open clusters [34]. Open clusters such as those discussed here suggest the interesting prospect of extension into tubular objects and potentially linkage of closed clusters through these to form porous frameworks.

3.2. Closed clusters with topological squares and hexagons

Only the U_{24} cluster has been found to have a topology that contains just squares and hexagons (Fig. 6a). We have obtained this cluster in hundreds of synthesis experiments with a variety of counter ions. The topology is elegantly simple, with each square in the topology sharing all four edges with hexagons. Hexagons share three edges with squares and the other three with adjacent hexagons. The resulting topology is well known as the silicate cage in the mineral sodalite and related materials [67].

3.3. Closed clusters with topological squares, pentagons and hexagons

The U_{32} and U_{40} clusters contain two topological squares and these are located at the ends of a somewhat elongated cluster in U_{40} (Fig. 6 b,c,e,f). In both clusters, each of the topological squares share all four of their edges with hexagons, identical to the U_{16} bowl-shaped cluster and fragments of the U_{24} cluster. In U_{32}, these U_{16}-like topological fragments are connected through a ring of edge-sharing pentagons (Fig. 6e). This results in a cluster composed of two topological squares, eight pentagons and eight hexagons. Each pentagon shares two of its edges with other pentagons and three with hexagons, two of which are from one U_{16}-like fragment. Hexagons share one edge with a topological square, two with other hexagons and three with pentagons.

In U_{40}, the linkage of the U_{16}-like clusters is significantly different from U_{32}. U_{40} also contains two topological squares and eight pentagons, but has twelve hexagons, four more than U_{32}. The arrangement of pentagons is very different in the two clusters. In U_{40}, pentagons occur in pairs with a shared edge (Fig. 6f). The long dimension of these pairs extends along the long axis of the cluster and each of the two pentagons shares two of its edges with hexagons of the U_{16}-like topological fragment. Hexagons separate four such pairs of pentagons, forming a ring consisting of four hexagons and eight pentagons. Each of these ring hexagons shares four edges with four different pentagons and one each with the hexagons of the two U_{16}-like cluster ends.

The U_{16} bowl-shaped cluster and the U_{24}, U_{32} and U_{40} closed clusters constitute a related family of topologies of progressively increasing complexity and size. The details of growth conditions that stabilize these different topologies remain unclear at this time and are the focus of ongoing research in our group.

3.4. Closed clusters with topological pentagons and hexagons (fullerene topologies)

Fullerenes, made famous by the discovery of C_{60} buckminsterfullerene [68] more than 20 years ago, are topologies containing 12 pentagons and an even number of hexagons. The smallest possible fullerene topology consists of 20 vertices and contains only 12 pentagons. Local curvature in a fullerene topology is related to the distribution of pentagons [69] and adjacent pentagons increase curvature and structural strain in the case of C fullerenes by decreasing orbital overlap [69]. To completely avoid adjacent pentagons in a fullerene topology, there must be at least 60 vertices. The most stable C fullerene, C_{60}, consists of 60 C atoms and adopts the only fullerene topology with 60 vertices that has no adjacent pentagons.

We recently identified four conditions that must be met in order for metal–oxygen isopolyhedra to assemble into fullerene topologies [31]:

1. Each polyhedron must link to exactly three other polyhedra and the most stable structures will occur when the connections between the metal–oxygen polyhedra are by the sharing of polyhedral edges.
2. The polyhedra must be geometrically compatible with forming topological pentagons and hexagons.
3. The three linkages emanating from any given polyhedron should be approximately coplanar to facilitate the cage geometry.
4. Linkages between polyhedra should be consistent with the bond-valence requirements of the shared polyhedral elements within the cage.

These conditions favor the self-assembly of hexagonal bipyramids into fullerene topologies. To date, we have reported the synthesis and structures of six different uranyl peroxide clusters with fullerene topologies. In stark contrast to the case of C-based fullerenes, there appears to be no energetic penalty associated with the presence of adjacent pentagons in such a topology. This is confirmed by the synthesis of the U_{20} cluster [32], which has the maximum possible pentagonal adjacencies (Fig. 7a,d). This is the only fullerene topology with 20 vertices. The cluster only contains uranyl triperoxide hexagonal bipyramids. Its diameter, measured from the edges of the bounding O atoms, is 18.0 Å [70].

Each of the U_{28}, U_{36}, U_{44}, U_{50} and U_{60} clusters, all of which have fullerene topologies, are shown in Fig. 7. The most remarkable of these are the U_{50} and U_{60} clusters owing to their size and complex topologies (Fig. 7 h,i,k,l). There are 271 fullerene topologies that contain 50 vertices and U_{50} adopts the one that has both the least pentagonal adjacencies and the highest symmetry. This is the same topology that is adopted by the "baby buckyball" $C_{50}Cl_{10}$ [71]. There are 1812 fullerene topologies that contain 60 vertices and U_{60} adopts the only one that has no pentagonal adjacencies. This topology also has the highest symmetry of the 1812 isomers. U_{60} and C_{60} buckminsterfullerene have identical topologies [33].

The U_{50} cluster contains only uranyl diperoxide dihydroxide polyhedra and is somewhat elongated. Measured from the edges of bounding O atoms, the cluster has a maximum length of 26.6 Å [31]. U_{60} contains 60 compositionally identical uranyl diperoxide dihydroxide polyhedra and its diameter, measured from the edges of the bounding O atoms, is 26.9 Å [33]. Synthesis requires

both K and Li counter ions, each of which occur inside the cluster. U_{60} is readily synthesized from aqueous solution at a pH of 9 at room temperature and can be precipitated into crystals that are several millimetres in diameter.

Each of the U_{28}, U_{36}, U_{50} and U_{60} clusters adopt the topology with the least pentagonal adjacencies. In each case, the topology with the least pentagonal adjacencies also has the highest symmetry. The U_{44} cluster, which is peanut-shaped, adopts a fullerene topology that does not have the least pentagonal adjacencies. Rather, a higher symmetry topology is utilized of the 89 possibilities with 44 vertices. We have argued that pentagonal adjacencies is not an important issue in the case of fullerene topologies built from uranyl polyhedra, but that higher symmetry is favored because such clusters have strain more evenly distributed [33].

3.5. Why clusters of uranyl peroxide polyhedra form

The mineral studtite provided the first inorganic structure in which uranyl hexagonal bipyramids are bridged by peroxide, and the peroxide group extends along the shared equatorial edge of the bipyramid [72]. This same type of linkage is present in all of the clusters of uranyl peroxide polyhedra we have reported. Sigmon et al. recently examined the geometries of these clusters, as well as fragments of the clusters isolated in crystal structures [70]. Using oxalate ligands to frustrate linkage of structure fragments into closed clusters, a dimer of uranyl peroxide polyhedra and both a five and six-membered ring of uranyl peroxide polyhedra were crystallized. In all cases, the dihedral angle of the U–O_2–U connection is strongly bent. Examination of previously published structures confirmed that where an edge consisting of two hydroxyl groups is shared between uranyl polyhedra, the U–$(OH)_2$–U dihedral angle is sometimes 180°. Where the bridge is peroxide, all of the known linkages have strongly bent U–O_2–U dihedral angles, which prompted Sigmon et al. to conclude that the U–O_2–U linkage is inherently bent [70]. The underlying cause of this conformation may be revealed by high-level simulations that are currently underway.

An inherently bent U–O_2–U linkage interrupts the tendency of uranyl polyhedra to link into infinite chains and favors the formation of clusters. This leads to the interesting prospect of tuning the U–O_2–U angles, perhaps using counter ions, to achieve specific uranyl peroxide cluster geometries.

4. Future directions

The systematic combinatorial synthesis campaign in search of clusters if uranyl peroxide polyhedra is complete and several additional clusters will be reported in forthcoming manuscripts. We are now turning our attention to detailed studies of the properties of uranyl peroxide clusters, with an emphasis on their energetics and aqueous solubilities. We are also systematically examining the evolution of cluster topologies in solution, as a function of solution conditions, using SAXS. We hope to gain an understanding of the relationships between the counter ions present and the cluster topology that forms and the properties of individual clusters relative to their topologies.

Acknowledgements

Much of this research was supported by the Chemical Sciences, Geosciences and Biosciences Division, Office of Basic Energy Sciences, Office of Science, U.S. Department of Energy, Grant No. DE-FG02-07ER15880.

References

[1] P.C. Burns, Can. Mineral. 43 (2005) 1839.
[2] T.Z. Forbes, C. Wallace, P.C. Burns, Can. Mineral. 46 (2008) 1623.
[3] L.R. Morss, N.M. Edelstein, J. Fuger, J.J. Katz, The chemistry of the actinide and transactinide elements, Springer, Dordrecht, 2006.
[4] P.C. Burns, R.C. Ewing, F.C. Hawthorne, Can. Mineral. 35 (1997) 1551.
[5] I.D. Brown, Phys. Chem. Miner. 15 (1987) 30.
[6] I.D. Brown, Acta Crystallogr. B 48 (1992) 553.
[7] I.D. Brown, D. Altermatt, Acta Crystallogr. B 41 (1985) 244.
[8] J.C. Sullivan, A.J. Zielen, J.C. Hindman, J. Amer. Chem .Soc. 83 (1961) 3373.
[9] N.N. Krot, M.S. Grigoriev, Russ. Chem. Rev. 73 (2004) 89.
[10] P.L. Arnold, J.B. Love, D. Patel, Coordination Chemistry Reviews 253 (2009) 1973.
[11] J.C. Berthet, G. Siffredi, P. Thuery, M. Ephritikhine, Chemical Communications (2006) 3184.
[12] J.C. Berthet, G. Siffredi, P. Thuery, M. Ephritikhine, Dalton Transactions (2009) 3478.
[13] F. Burdet, J. Pecaut, M. Mazzanti, Journal of the American Chemical Society 128 (2006) 16512.
[14] V. Mougel, P. Horeglad, G. Nocton, J. Pecaut, M. Mazzanti, Angewandte Chemie-International Edition 48 (2009) 8477.
[15] G. Nocton, P. Horeglad, J. Pecaut, M. Mazzanti, Journal of the American Chemical Society 130 (2008) 16633.
[16] L.P. Spencer, E.J. Schelter, P. Yang, R.L. Gdula, B.L. Scott, J.D. Thompson, J.L. Kiplinger, E.R. Batista, J.M. Boncella, Angewandte Chemie-International Edition 48 (2009) 3795.
[17] P.C. Burns, M.L. Miller, R.C. Ewing, Can. Mineral. 34 (1996) 845.
[18] R.J. Finch, R.C. Ewing, J. Nucl. Mater. 190 (1992) 133.
[19] E.C. Buck, N.R. Brown, N.L. Dietz, Environmental Science & Technology 30 (1996) 81.
[20] E.C. Buck, N.L. Dietz, J.K. Bates, Microscopy Research and Technique 31 (1995) 174.
[21] S.F. Wolf, J.K. Bates, E.C. Buck, N.L. Dietz, J.A. Portner, N.R. Brown, Environmental Science & Technology 31 (1997) 467.
[22] P.C. Burns, K.M. Deely, S. Skanthakumar, Radiochim. Acta 92 (2004) 151.
[23] P.C. Burns, P.C. Ewing, M.L. Miller, J. Nucl. Mater. 245 (1997) 1.
[24] M. Douglas, S.B. Clark, J.I. Friese, B.W. Arey, E.C. Buck, B.D. Hanson, Environ. Sci. Technol. 39 (2005) 4117.
[25] M. Douglas, S.B. Clark, J.I. Friese, B.W. Arey, E.C. Buck, B.D. Hanson, S. Utsunomiya, R.C. Ewing, Radiochim. Acta 93 (2005) 265.
[26] J. A. Fortner, R. J. Finch, A. J. Kropf, J. C. Cunnane, Nuclear Technology 148 (2004) 174–180.
[27] C.W. Kim, D.J. Wronkiewicz, R.J. Finch, E.C. Buck, Journal of Nuclear Materials 353 (2006) 147.
[28] D.J. Wronkiewicz, J.K. Bates, T.J. Gerding, E. Veleckis, B.S. Tani, Journal of Nuclear Materials 190 (1992) 107.
[29] D. J. Wronkiewicz, J. K. Bates, S. F. Wolf, E. C. Buck, Journal of Nuclear Materials 238 (1996) 78–95.
[30] P.C. Burns, K.A. Kubatko, G. Sigmon, B.J. Fryer, J.E. Gagnon, M.R. Antonio, L. Soderholm, Angew. Chem. - Int. Ed. 44 (2005) 2135.
[31] T.Z. Forbes, J.G. McAlpin, R. Murphy, P.C. Burns, Angew. Chem. - Int. Ed. 47 (2008) 2824.
[32] G. Sigmon, J. Ling, D.K. Unruh, L. Moore-Shay, M. Ward, B. Weaver, P.C. Burns, J. Amer. Chem . Soc (2010).
[33] G.E. Sigmon, D.K. Unruh, J. Ling, B. Weaver, M. Ward, L. Pressprich, A. Simonetti, P.C. Burns, Angew. Chem. - Int. Ed. 48 (2009) 2737.
[34] G.E. Sigmon, B. Weaver, K.A. Kubatko, P.C. Burns, Inorg. Chem. 48 (2009) 10907.
[35] L. Soderholm, P.M. Almond, S. Skanthakumar, R.E. Wilson, P.C. Burns, Angewandte Chemie-International Edition 47 (2008) 298.
[36] T.Z. Forbes, P.C. Burns, J. Solid State Chem. 178 (2005) 3445.
[37] T.Z. Forbes, P.C. Burns, Amer. Mineral. 91 (2006) 1089.
[38] T.Z. Forbes, P.C. Burns, Can. Mineral. 45 (2007) 471.
[39] T.Z. Forbes, P.C. Burns, J. Solid State Chem. 180 (2007) 106.
[40] T.Z. Forbes, P.C. Burns, Inorg. Chem. 47 (2008) 705.

[41] T.Z. Forbes, P.C. Burns, J. Solid State Chem (2008).
[42] T.Z. Forbes, P.C. Burns, S. Skanthakumar, L. Soderholm, J. Amer. Chem. Soc. 129 (2007) 2760.
[43] T.Z. Forbes, P.C. Burns, L. Soderholm, S. Skanthakumar, Chem. Mater. 18 (2006) 1643.
[44] R.E. Wilson, P.M. Almond, P.C. Burns, L. Soderholm, Inorganic Chemistry 45 (2006) 8483.
[45] P.C. Burns, L.A. Hayden, Acta Crystallogr. C 58 (2002) I121.
[46] L.A. Hayden, P.C. Burns, J. Solid State Chem. 163 (2002) 313.
[47] L.A. Hayden, P.C. Burns, Canadian Mineralogist 40 (2002) 211.
[48] S.V. Krivovichev, P.C. Burns, Canadian Mineralogist 39 (2001) 197.
[49] S.V. Krivovichev, P.C. Burns, Canadian Mineralogist 41 (2003) 707.
[50] P.C. Burns, Canadian Mineralogist 39 (2001) 1139.
[51] S.V. Krivovichev, P.C. Burns, Zeit. Kristallogr. 218 (2003) 725.
[52] P.C. Burns, American Mineralogist 84 (1999) 1661.
[53] Y.P. Li, P.C. Burns, R.A. Gault, Canadian Mineralogist 38 (2000) 153.
[54] N.N. Krot, M.S. Grigoriev, Uspekhi Khimii 73 (2004) 94.
[55] Y.P. Li, P.C. Burns, Canadian Mineralogist 38 (2000) 1433.
[56] A.J. Locock, P.C. Burns, Journal of Solid State Chemistry 163 (2002) 275.
[57] K.A. Kubatko, P.C. Burns, Inorg. Chem. 45 (2006) 10277.
[58] P.M. Almond, S. Skanthakumar, L. Soderholm, P.C. Burns, Chem. Mater. 19 (2007) 280.
[59] J. Cejka, J. Sejkora, M. Deliens, Neues Jahrbuch Fur Mineralogie-Monatshefte (1996) 125.
[60] K. Walenta, American Mineralogist 59 (1973) 166.
[61] K.A.H. Kubatko, K.B. Helean, A. Navrotsky, P.C. Burns, Science 302 (2003) 1191.
[62] B.E. Burakov, E.E. Stykanova, E.B. Anderson, Mater. Res. Soc. Proc. (1997) 757.
[63] B.B. McNamara, Mater. Res. Soc. Proc. 757 (2002) 401.
[64] B.B. McNamara, Radiochim. Acta 93 (2005) 169.
[65] I. I. Chernyaev, Complex compounds of uranium; Academy of Sciences of the U.S.S.R. (1966).
[66] N.W. Alcock, J. Chem.Soc. A - Inorg. Phys. Theor. (1968) 1588.
[67] C. Baerloch, W.M. Meier, Helvetica Chimica Acta 52 (1969) 1853.
[68] H.W. Kroto, J.R. Heath, S.C. Obrien, R.F. Curl, R.E. Smalley, Nature 318 (1985) 162.
[69] P. Fowler, D. Manolopoulos, An atlas of fullerenes;, 2nd ed, Dover Publications, Inc, Mineola, New York, 2006.
[70] G. Sigmon, J. Ling, D.K. Unruh, L. Moore-Shay, M. Ward, B. Weaver, P.C. Burns, J. Amer. Chem .Soc. 131 (2009) 16648.
[71] S.Y. Xie, F. Gao, X. Lu, R.B. Huang, C.R. Wang, X. Zhang, M.L. Liu, S.L. Deng, L.S. Zheng, Science 304 (2004) 699.
[72] P.C. Burns, K.A. Hughes, Amer. Mineral. 88 (2003) 1165.